HHS Public Access

Author manuscript

Nat Immunol. Author manuscript; available in PMC 2013 January 18.

Published in final edited form as:

Nat Immunol. ; 13(7): 681–690. doi:10.1038/ni.2309.

Regulation of T_H2 development by CXCR5$^+$ dendritic cells and lymphotoxin-expressing B cells

Beatriz León[1,3], **André Ballesteros-Tato**[1,3], **Jeffrey L. Browning**[2], **Robert Dunn**[2,4], **Troy D. Randall**[1,5], and **Frances E. Lund**[1,3,6]

[1]University of Rochester Medical Center, Dept. of Medicine, Division of Allergy, Immunology and Rheumatology, Rochester NY USA

[2]Biogen Idec, Cambridge MA USA and San Diego CA USA

Abstract

Although cognate encounters between CCR7-expressing antigen-bearing dendritic cells (DCs) and CCR7$^+$ naïve T cells take place within the T cell zone of lymph nodes, it is unknown whether co-localization of the DCs and T cells within the T cell area is obligate for effector generation. Here, we show that, following nematode infection, antigen-bearing DCs and CD4$^+$ T cells upregulate CXCR5 and co-localize in a CXCL13, B cell and lymphotoxin-dependent fashion outside of the T zone. Importantly, lymphotoxin-expressing B cells, CXCL13 and CXCR5-expressing DCs and T cells are also necessary for development of interleukin 4 (IL-4) producing T_H2 cells, suggesting that T_H2 differentiation can initiate outside of the T cell zone.

Introduction

According to the current paradigm[1,2] naïve CCR7$^+$ T cells and antigen-bearing mature CCR7$^+$ dendritic cells (DCs) enter lymph nodes (LNs) and migrate in a CCL19-dependent fashion to the T cell zone where antigen-specific encounters and T cell priming takes place. However, *plt/plt* mice[3] which lack the CCR7 ligands, CCL19 and CCL21a, can make normal or even enhanced CD4$^+$ T cell responses[4,5], suggesting that DC-dependent priming of some CD4$^+$ T cell responses may occur outside the T zone. Indeed, emerging evidence suggests that T cells and DCs may also have the opportunity to engage one another in the B cell area. For example, T follicular helper (T_{FH}) cells[6–8] and some DCs in the marginal zone of the spleen[9] and the dermis of the skin[10] express CXCR5 and localize near the CXCR5$^+$ B

[6]Correspondence addressed to: flund@uab.edu Univ. Alabama Birmingham, Dept. Microbiology, 1530 3rd Ave South BBRB 276/11, Birmingham AL 35294-2170.

[3]Current Address: University of Alabama at Birmingham, Dept. of Microbiology, Birmingham AL USA

[4]Current Address Pfizer-Centers for Therapeutic Innovation, San Diego CA

[5]Current Address: University of Alabama at Birmingham, Div. of Clinical Immunology and Rheumatology, Birmingham AL USA

Author contributions. B.L., A.B-T., F.E.L. and T.D.R. each contributed to the design of the experiments and the writing of the manuscript. B.L. performed all experiments with help from A.B-T. J.B. and R.D. provided advice, discussion and reagents that were critical to this work. All authors reviewed the manuscript before submission.

Competing financial interests. R. Dunn and J. Browning are (JB) or have been (RD) employees of Biogen Idec which has a financial interest in anti-CD20 therapy for humans. The other authors declare no financial conflicts of interest related to this work.

cells and the stromal-derived follicular dendritic cells (FDCs)[11,12], and marginal reticular cells (MRCs)[13]. These stromal cell subsets, which are located below the subcapsular sinus (SCS), within the B cell follicles and in the inter- and perifollicular regions between the B cell follicles, express CXCL13 and can attract or retain CXCR5-expressing cells. Although it makes sense that T_{FH} development, which is dependent on antigen-presenting DCs and B cells[14–16], might take place near B cell follicles, it is less obvious whether other types of CD4 effector responses can be initiated in the B cell area of the LN.

Here we show that a population of CXCR5-expressing DCs that migrate to the LN and localize adjacent to B cell follicles are induced in mice infected with the intestinal nematode, *Heligmosomoides polygyrus* (*Hp*). Deletion of CXCR5 in either DCs or the $CD4^+$ T cells prevents the co-localization of the DCs and $CD4^+$ T cells near the B cell area and impairs both T_{FH} and T_H2 effector development. Interestingly, lymphotoxin (LT)-expressing B cells control CXCL13 transcription and regulate the CXCL13-dependent positioning of the DCs and T cells in the LN. Most importantly, T_H2 effector responses in the LN and peripheral tissues are substantially impaired in mice treated with therapeutics that either cause transient B cell depletion or that block LT or CXCL13 signaling. Thus, *Hp*-induced IL-4-expressing T_{FH} and T_H2 effector cell responses are initiated in a CXCL13, LT and B cell dependent fashion within an specialized microenvironment outside of the T zone.

Results

Hp infection alters DC chemokine receptor expression

Mature DCs typically localize within the T cell zone of the LN[17,18]. However $CXCR5^+$ DC populations have been identified and found to localize near B cell follicles[9,10]. To determine whether we could detect DCs that preferentially localize near B cells following different types of infections, we determined the localization of the DCs in either the mediastinal LN (medLN) of influenza-infected C57BL/6J (B6) mice or the mesenteric LN (mesLN) of mice infected with the nematode *Hp.* As expected, $CD11c^+$ DCs were predominantly found in the T cell areas of the uninfected animals (Fig. 1a). Similarly, medLN $CD11c^+$ DCs from influenza-infected mice were also found primarily in the T cell area (Fig. 1a). By contrast, $CD11c^+$ DCs in the mesLNs of *Hp*-infected mice were observed below the SCS, in the interfollicular areas and at the T:B border (Fig. 1a,b). Thus, DCs accumulate in different regions of the LN following influenza and *Hp* infections.

Given the unexpected positioning of the $CD11c^+$ cells within the mesLN of *Hp*-infected mice, we phenotypically and functionally characterized the $CD11c^+$ DCs in the LN on day 8 – at the peak of the DC response (Supplementary Fig. 1a). We identified two major populations of DCs – the $MHCII^+CD40^{hi}CD11c^{int}DEC205^+$ mature DCs and the $MHCII^{lo}CD40^{lo}CD11c^{hi}DEC205^-$ immature DCs (Fig. 2a,b). As expected, the number of the mature mesLN DCs increased 8–10 fold following *Hp* infection (Supplementary Fig. 1a). Importantly, we identified similar migratory DC subsets in the medLN of influenza-infected mice[19] (Supplementary Fig. 1b-i).

Since the $MHCII^+CD11c^{int}CD40^{hi}DEC205^+$ DCs in the medLN of influenza-infected mice present influenza antigens[19], we postulated that the corresponding DCs in the mesLN of *Hp*-

infected mice would present *Hp* antigens to T cells. We therefore sorted MHCII^{+}CD11c^{int} mature DCs and MHCII^{lo}CD11c^{hi} immature DCs from the mesLN of day 8 *Hp*-infected mice, co-cultured them with CD4^{+} T cells purified from mesLN of day 5 *Hp*-infected IL-4 reporter mice[20] and measured the *in vitro* expansion of the IL-4 mRNA expressing (EGFP^{+}) T cells. Approximately 10% of the input CD4^{+} T cells expressed EGFP before culture with DCs (Fig. 2c). The EGFP^{+} T cells expanded 10-fold when co-cultured with mature DCs from *Hp*-infected mice (Fig. 2c,d), suggesting that these phenotypically mature DCs are competent to present *Hp* antigen and expand *Hp*-specific CD4^{+} T cells.

Next, we compared CCR7 and CXCR5 expression on immature (MHCII^{lo}CD11c^{hi}CD40^{lo}) and mature (MHCII^{+}CD11c^{int}CD40^{hi}) DCs from the mesLNs or medLNs of uninfected, influenza-infected or *Hp*-infected mice. As expected, the vast majority of the immature DCs were CCR7 and CXCR5 negative (Fig. 2e). However, ~80% of the mature DCs from the uninfected medLN and mesLNs and from the medLN of influenza-infected mice (Fig. 2f-h) expressed CCR7. By contrast, only 25–30% of the mature DCs from the mesLNs of *Hp*-infected mice expressed detectable amounts of CCR7 (Fig. 2g,h). Instead, the majority of these DCs expressed CXCR5 (Fig. 2g,h), either alone or in combination with CCR7 (Supplementary Fig. 2a).

To determine whether mature DCs from *Hp*-infected mice were altered in their ability to respond to CCR7 and CXCR5 ligands, we performed *in vitro* chemotaxis assays. Immature DCs did not migrate to CCL19 or CXCL13 (Fig. 2i), while mature LN DCs from uninfected or influenza-infected mice responded to CCL19, but only marginally to CXCL13 (Fig. 2j). Conversely, mature DCs from *Hp*-infected mice exhibited increased migration to CXCL13 and diminished migration to CCL19 (Fig. 2j). In fact, the percentage of mature DCs capable of migrating to CCL19 declined from 22% to 8% following *Hp* infection while the percentage of DCs that migrated to CXCL13 more than doubled from 3% to 8% (Supplementary Fig. 2b). Not surprisingly, given the lower CXCL13 expression in mature DCs relative to B cells (Supplementary Fig. 2c), the mature DCs from *Hp*-infected mesLNs did not migrate as effectively to CXCL13 as the B cells from the same LN (Supplementary Fig. 2d-e). Regardless, the antigen-bearing migratory mesLN DCs from *Hp*-infected mice clearly exhibited altered responsiveness to chemokines that control the positioning of cells within the LN.

T_H2 responses to *Hp* are regulated by CXCL13 but not CCL19

Given the altered responsiveness of the mature DCs from *Hp*-infected mice to CCL19 and CXCL13, we postulated that the development of T_H2 responses to *Hp* might be less reliant on CCR7 ligands and more dependent on CXCR5 ligands. To test this hypothesis, we first evaluated T cell responses in *Hp*-infected CCL19-deficient *plt/plt* mice. As expected[3], the number of mature DCs was decreased in the mesLN of naïve *plt/plt* mice (Supplementary Fig. 3a,b). However, by 8 days post-*Hp* infection, the frequencies and numbers of immature and mature mesLN DCs were equivalent between the B6 and *plt/plt* mice (Fig. 3a,b). Furthermore, the DCs in both groups of mice were found below the SCS and in the interfollicular areas (Fig. 3c). More importantly, both the frequency and number of CD4^{+} T cells that produced IL-4 following restimulation were almost identical in the *plt/plt* and B6

mice (Fig. 3d,e), indicating that CCL19 was not required for *Hp*-dependent T_H2 development.

Next, we treated mice with control or CXCL13-specific antibodies at the time of *Hp* infection and examined the DC and T cell response 8 days later. CXCL13 blockade had no effect on LN cellularity or on the number of immature and mature DCs in the reactive LN (Fig. 3f). However, DCs in anti-CXCL13-treated mice localized within the T cell area rather than near the B cell follicles (Fig. 3g). Despite the presence of the DCs in the T zone of the anti-CXCL13 treated mice, the frequency and number of mesLN $CD4^+$ T cells that produced IL-4 following restimulation were significantly decreased (Fig. 3h,i). Similar results were observed in *Hp*-infected *Cxcl13*$^{-/-}$ (ref. 21) and *Cxcr5*$^{-/-}$ mice[22] (Fig. 3h,i). Interestingly, the frequency and number of IL-4 producing T_H2 cells present in a peripheral site, the peritoneal cavity (PEC), were also significantly decreased in the anti-CXCL13 treated group (Fig. 3j,k). By contrast, anti-CXCL13 treatment did not impair the development of IFN-γ-producing T_H1 cells following influenza infection (Fig. 3l,m). Therefore, although CXCL13 is important for the development of a *Hp*-specific T_H2 response in the LN and periphery, it is dispensable for the development of a T_H1 response to influenza.

CXCR5$^+$ DCs regulate *Hp*-induced T_H2 development

To test whether T_H2 responses to *Hp* are dependent on CXCR5-expressing DCs, we reconstituted irradiated B6 recipients with an 80:20 mix of bone marrow (BM) from CD11c-diphtheria toxin receptor mice (CD11c-DTR)[23] and *Cxcr5*$^{-/-}$ mice (DC-*Cxcr5*$^{-/-}$ chimeras – Supplementary Fig. 4) or with an 80:20 mix of BM from CD11c-DTR mice and B6 mice (DC-WT chimeras – Supplementary Fig. 4). Following reconstitution, we treated both groups with diphtheria toxin (DT) to ablate the $CD11c^+$ cells derived from the CD11c-DTR BM. We then transferred purified naïve $CD4^+$ T cells from B6.$CD45.1^+$ mice into both groups of chimeras and infected the mice with *Hp*. Although the frequency (Fig. 4a) and number (not shown) of mesLN DCs were similar in both groups of mice, the majority of responding DCs remaining in the DT-treated *Hp*-infected DC-WT chimeras expressed CXCR5, while the responding DCs from DC-*Cxcr5*$^{-/-}$ chimeras were largely CXCR5 negative (Fig. 4b). DCs from *Hp*-infected DC-WT chimeras were positioned in the interfollicular regions (Fig. 4c), whereas DCs from *Hp*-infected DC-*Cxcr5*$^{-/-}$ chimeras accumulated mostly in the T zone (Fig. 4c). Interestingly, the frequency and number IL-4 producing wild-type $CD45.1^+$ $CD4^+$ T cells present in the mesLN (Fig. 4d,e) and PEC (Fig. 4f,g) of the DC-*Cxcr5*$^{-/-}$chimeras were significantly decreased relative to those in DC-WT chimeras. Thus, CXCR5 expression by $CD11c^+$ cells controlled the positioning of DCs within the infected LN and was also necessary for the development of maximal T_H2 responses in LN and peripheral sites.

T_{FH} and T_H2 development requires CXCR5$^+$ T cells

Our data suggested that *Hp*-induced T_H2 responses might also be dependent on a CXCR5-expressing T cell population. To address this possibility, we examined CXCR5 expression on T_{FH} and T_H2 cells from day 8 *Hp*-infected IL-4 reporter mice. Using PD-1 we subdivided the IL-4 committed ($EGFP^+$) $CD44^{hi}ICOS^+$ $CD4^+$ T cells into PD-1^{hi} T_{FH} and PD-1^{lo} T_H2 subpopulations (Fig. 5a). As expected, PD-1^{lo} T_H2 cells produced both IL-4

(Fig. 5b) and IL-13 (Supplementary Fig. 5a) following restimulation and were found in peripheral sites like the PEC (Supplementary Fig. 5b). By contrast the PD-1^{hi} T_{FH} population was not detected in the PEC of *Hp*-infected mice (Supplementary Fig. 5b) or in the LNs of *Hp*-infected B cell-deficient IL-4-reporter mice (Supplementary Fig. 5c). None of the restimulated PD-1^{hi} T_{FH} cells produced IL-13 (Supplementary Fig. 5a) and only a small fraction made IL-4 (Fig. 5b). However, as expected, PD-1^{hi} T_{FH} cells expressed abundant CXCR5 and intracellular Bcl6 (Fig. 5c,d and Supplementary Fig. 5d). Surprisingly, the EGFP^{+}PD-1^{lo} T_H2 cells in the mesLN also expressed CXCR5 and Bcl6, albeit in lower amounts than observed in the T_{FH} cells (Fig. 5c,d and Supplementary Fig. 5d).

Since both T_{FH} and T_H2 cells in *Hp*-infected mesLNs expressed CXCR5, we expected to find these cells localized in a CXCL13-dependent fashion near B cell follicles. Using anti-CD8 to define the T cell zone and anti-B220 to define B cell follicles, we first examined the positioning of the CD4^{+} T cells and CD11c^{+} DCs in *Hp*-infected mesLNs. Some CD4^{+} T cells co-localized with the CD8^{+} T cells in the T zone. However, unlike the CD8^{+} T cells, CD4^{+} T cells were also present in the perifollicular area and B cell follicles (Fig. 5e). Following anti-CXCL13 treatment, CD4^{+} T cells no longer accumulated in the perifollicular region and instead accumulated in the T cell area (Fig. 5f). Despite anti-CXCL13 treatment facilitating co-localization of the CD4^{+} T cells and DCs in the T zone, the numbers of ICOS^{+}PD-1^{hi} T_{FH} cells (Fig. 5g) and IL-4-producing ICOS^{+}PD-1^{lo} T_H2 cells (Fig. 5h) were significantly decreased.

To address whether CXCR5-expressing T cells are necessary for *Hp*-induced T_H2 and T_{FH} development, we reconstituted irradiated B6.CD45.1^{+} recipients with a 50:50 mixture of B6.CD45.1^{+} BM and *Cxcr5*$^{-/-}$ (CD45.2^{+}) BM (Supplementary Fig. 6). We infected the reconstituted chimeric mice with *Hp* and determined the frequencies of B6 (CD45.1^{+}) and *Cxcr5*$^{-/-}$ (CD45.2^{+}) cells within the mesLN and PEC on day 8 post-infection. The percentages of total B6 and *Cxcr5*$^{-/-}$ mesLN cells were equivalent in the chimeras (Fig. 5i) and the frequencies of naïve CD44^{lo}CD4^{+} T cells from both genotypes were identical (Fig. 5j). However, the percentages of *Cxcr5*$^{-/-}$ ICOS^{+}PD-1^{hi} T_{FH} cells and *Cxcr5*$^{-/-}$ ICOS^{+}PD-1^{lo} effectors were significantly decreased compared to the equivalent populations of B6 cells (Fig. 5j). Strikingly, the percentages of IL-4-producing *Cxcr5*$^{-/-}$ CD4^{+} T cells in the mesLN (Fig. 5k) and PEC (Fig. 5l) were also significantly lower than the percentage of IL-4-producing B6 T cells in these tissues. Therefore, optimal development of LN T_{FH} responses and LN and peripheral T_H2 responses to *Hp* were dependent on a CXCR5-expressing T cell population.

B cell depletion impairs T_{FH} and T_H2 development

Given that CXCR5 expression by both CD4^{+} T cells and DCs was required for maximal T_{FH} and T_H2 responses to *Hp*, we reasoned that co-localization of B cells with DCs or CD4^{+} T cells may be necessary for optimal T_H2 generation. To test this, we treated B6 mice with control antibody or B cell depleting anti-CD20 4 days before infection with *Hp* and, on day 8 post-infection, we evaluated the architecture of the mesLN and the CD4^{+} T cell response. In control mice, DCs and CD4^{+} T cells were positioned in close proximity to the B cells

(Fig. 6a and Supplementary Fig. 7). By contrast, in the anti-CD20–treated group, B cell follicles were ablated (Fig. 6b) and the DCs and $CD4^+$ T cells were disorganized and found throughout the LN (Fig. 6a,b and Supplementary Fig. 7). As expected, the number of $ICOS^+PD\text{-}1^{hi}$ T_{FH} cells was significantly reduced in B cell-depleted mice (Fig. 6c). However, the frequencies and numbers of $ICOS^+PD\text{-}1^{lo}$ IL-4 (Fig. 6d,e) and IL-13-producing (Supplementary Fig. 8a,b) T_H2 cells in the LN (Fig. 6d,e) and $IL\text{-}4^+$ $CD4^+$ T cells in PEC (Supplementary Fig. 8c,d) were also significantly decreased in B cell-depleted mice. Similar results were observed in *Hp*-infected MD4μMT mice, which express a monoclonal repertoire of transgenic B cells specific for an irrelevant antigen (Supplementary Fig. 8e-g). As a control, we also infected anti-CD20 treated, B cell-depleted mice with influenza and determined the number of nucleoprotein (NP)-specific $ICOS^+PD\text{-}1^{hi}$ T_{FH} and $ICOS^+PD\text{-}1^{lo}$ effector T cells in the medLN on day 8. Although B cell depletion suppressed the NP-specific T_{FH} response (Fig. 6f), it had no effect on the day 8 NP-specific IFN-γ-producing $CD4^+$ T_H1 response (Fig. 6g,h). Thus, B cells and CXCL13 were dispensable for the development of a primary T_H1 response to influenza, but necessary for the generation of an optimal T_H2 response to *Hp*.

LT regulates CXCL13 expression and T_H2 development

CXCL13 expression by stromal cells in the spleen is controlled by lymphotoxin (LT)-expressing B cells[24]. To address whether LT-expressing B cells might regulate the CXCR5-dependent T_H2 response by controlling CXCL13 expression in the mesLNs, we first examined membrane LT expression in the mesLNs following *Hp* infection. Although LT was only marginally expressed by mesLN T cells (Supplementary Fig. 9a), LT was detected on a fraction of mesLN B cells from uninfected mice (Fig. 7a) and was upregulated following *Hp* infection (Fig. 7b) on activated (FAS^+PNA^{lo}) and $PNA^{hi}FAS^+$ germinal center B cells (Supplementary Fig. 9b). Interestingly, neither non-specific B cells from BCR transgenic MD4μMT mice (Fig. 7c) nor B cells from DC-depleted CD11c-DTR mice (Fig. 7d) upregulated LT following *Hp* infection.

Next, to determine whether CXCL13 expression in the LNs of *Hp*-infected mice was controlled by LT or B cells, we treated mice with anti-CD20 or with a blocking LTβR-Fc fusion protein, infected the mice with *Hp* and quantified CXCL13 mRNA in the mesLN. CXCL13 expression in the mesLNs was significantly lower in B cell-depleted and in LTβR-Fc-treated mice compared to controls (Fig. 7e).

Finally, we treated mice with LTβR-Fc at the time of *Hp* infection and then examined the positioning of DCs and $CD4^+$ T cells in the LN and the development of the *Hp*-induced T_H2 response. Neither the frequency nor the number of mature DCs was affected by the LTβR-Fc treatment (Fig. 7f,g). Although LTβR-Fc treatment did not ablate the B cell follicles (Fig. 7h,i), DCs and $CD4^+$ T cells in the LTβR-Fc-treated mice no longer accumulated in the interfollicular areas and were instead found mostly in the T cell areas of the LN (Fig. 7h,i and Supplementary Fig. 10). Furthermore, the number of IL-4-producing T cells was significantly reduced in the LTβR-Fc treated *Hp*-infected mice compared to controls (Fig. 7j). Thus, CXCL13, B cells and LT were each required for the proper positioning of DCs

and T cells near the B cell follicles following *Hp* infection and were also required for optimal T_H2 development.

B cell-derived LT controls T_H2 responses to *Hp*

Collectively, our data suggested that LT, produced by B cells, regulates CXCL13 expression, and thereby controls the positioning of DCs and T cells within the mesLN and the development of an *Hp*-specific T_H2 response. To test this model, we generated 80:20 mixed BM chimeras in which B cells were either LT-deficient[25] (B-*Lta*$^{-/-}$ chimeras) or LT-sufficient (B-WT chimeras) (Supplementary Fig. 11). We infected the chimeric mice with *Hp* and evaluated the DC response, CXCL13 expression and the T_H2 response in the mesLN on day 8 post-infection. The numbers of mature and immature DCs in the mesLN of *Hp*-infected B-*Lta*$^{-/-}$ chimeras were equivalent to those found in B-WT chimeras (Fig. 8a,b). While DCs from *Hp*-infected B-WT chimeras were found adjacent to the B cell follicles (Fig. 8c), DCs from B-*Lta*$^{-/-}$ chimeras largely accumulated in the T cell area with the CD4$^+$ T cells (Fig. 8d). Consistent with these results, CXCL13 mRNA expression was reduced in *Hp*-infected B-*Lta*$^{-/-}$ chimeras relative to that in B-WT chimeras (Fig. 8e). Furthermore, the frequency and number of CD4$^+$ T cells able to produce IL-4 following restimulation were significantly less in B-*Lta*$^{-/-}$ chimeras compared to those in B-WT chimeras (Fig. 8f,g). Taken altogether, these data argue that *Hp*-induced T_H2 and T_{FH} responses develop in a CXCL13-dependent manner outside of the T cell zone and are regulated by CXCR5-expressing DCs and LT-expressing B cells.

Discussion

Although current models suggest that naïve T cells are first primed by antigen-bearing DCs in the T cell zone[17,26,27], we show that optimal development of *Hp*-induced T_{FH} and T_H2 cells requires CXCR5, CXCL13 and LT and appears to take place outside of the T zone, adjacent to B cell follicles. In fact, anti-CXCL13 and LTβR-Fc treatment, which impair T_H2 development to *Hp*, do not prevent co-localization of the CD4$^+$ T cells and DCs in the T zone, but do prevent these cells from accumulating near the B cell follicles. Thus, T_H2 responses to *Hp* are not only dependent on DC:T cell interactions but are also controlled by the microenvironment where these interactions occur.

The data indicate that expression of CXCR5 by DCs is required for optimal T_{FH} and T_H2 responses to *Hp*. Although activated DCs typically upregulate CCR7 (ref. 18), we found very few CCR7$^+$CXCR5$^-$ DCs following *Hp* infection. Instead, we identified populations of CXCR5$^+$CCR7$^-$ and CXCR5$^+$CCR7$^+$ mature DCs. Some of these DCs are responsive, at least *in vitro*, to CCL19 and CXCL13. Although these *Hp*-induced DCs are less responsive to CXCL13 than B cells, the DCs are also less responsive to CCL19 than the “prototypic” mature DCs from influenza-infected mice. This dual, but modest, responsiveness to CCR7 and CXCR5 ligands appears sufficient for the migratory DCs to reach the LN. However, once the DCs enter the LN through the SCS, the DCs first encounter CXCL13 that may provide a retention signal and prevents the DCs, which are only modestly responsive to CCL19, from migrating to the T cell area. CXCR5-expressing DCs were previously identified in the marginal zone of the spleen and the dermis of the skin[9,10]. While the

function of these DCs was not evaluated, the CXCR5$^+$ skin-derived DCs responded to CXCL13 and migrated to the B cell area of the LN upon adoptive transfer[10]. Furthermore, the marginal zone CXCR5$^+$ DCs disappeared in mice lacking B cells or LT[9]. Thus, these splenic and skin-derived populations of DCs may be quite similar to the CXCR5-expressing DC population induced upon *Hp* infection.

CXCR5 expression by T cells is also required for optimal T_{FH} and T_H2 responses to *Hp*. Although T_{FH} cells express CXCR5 (refs. 6–8), a role for CXCR5 in T_H2 development has not been evaluated. We found a population of CXCR5 and Bcl6-expressing mesLN T cells that also exhibited the phenotypic and functional hallmarks of bona fide IL-4 and IL-13 committed T_H2 cells[28]. Given that both the T_{FH} and T_H2 cells in the mesLNs of *Hp*-infected mice express IL-4 mRNA and Bcl6 and require B cells and CXCL13 for their optimal development, it appears that *Hp*-induced T_{FH} and T_H2 cell differentiation are linked. In support of this conclusion, T_{FH} and T_H2 cells responding to *Schistosoma mansoni* egg antigens are reported to arise from a common precursor[29]. Similarly, it was recently reported that T_H1 differentiation is marked by a T_{FH} cell-like transition[30]. Our data further argue that the development of this common T_{FH}-T_H2 precursor is controlled, in part, by the unique microenvironment in which the cells are located. We speculate that naïve *Hp*-specific T cells that enter the LN near B cell follicles are detained at this site by the CXCR5$^+$ antigen-presenting DCs and are directed to activate the transcription networks that control T_{FH}[7, 8] and T_H2 differentiation[28]. T cells that receive reinforcing signals from the nearby antigen-presenting B cells can maintain expression of Bcl6 and CXCR5 and become fully committed T_{FH} cells[14–16] that retain their capacity to produce IL-4 (refs. 29,31). By contrast, those T cells that do not interact with antigen-presenting B cells lose Bcl6 and CXCR5 expression[14–16] and become fully committed T_H2 cells that can eventually leave the LN and migrate peripheral effector sites.

One unique feature of the microenvironment where T_{FH} and T_H2 cells develop is the presence of B cells. Our data showing that B cells regulate T_H2 and T_{FH} development following *Hp* infection are consistent with results showing that B cells maintain T_{FH} responses[14–16], regulate the magnitude of primary T_H2 responses[32–35] and facilitate the development and maintenance of memory T_H2 cells[32,34]. Our data show that one way in which B cells modulate the development of T_{FH} and T_H2 effectors is by ensuring that CXCL13 is abundantly expressed in the B cell area of the reactive LN, thereby enhancing the retention of the CXCR5$^+$ DCs and CD4$^+$ T cells in this location. Given our data showing that B cells control CXCL13 abundance in a LT-dependent fashion in the LN, we speculate that the LT-expressing B cells communicate with the nearby LTβR-expressing stromal cells[24,36–38] and induce these cells to produce more CXCL13, allowing for more effective retention of the CXCR5-expressing DCs. This infection-induced response in the LN appears similar to the homeostatic feedback loop by which LT-expressing B cells organize the T cell area and the CXCL13-expressing FDCs in the spleen[21,39].

It is not immediately obvious why T_{FH} and T_H2 dependent responses to *Hp* are more effective when T cells and DCs co-localize in the perifollicular area, rather than in the T cell zone. One possibility is that B cells that present antigen and express cytokines or costimulatory molecules may be needed to drive T_H2 and T_{FH} cell differentiation.

Alternatively, other cells, such as macrophages that line the SCS and transfer antigens to B cells, also populate the perifollicular area[40,41] and may contribute to the process. It is also possible that IL-4 producing cells such as mast cells[28], which can express CXCR5 (ref. 42), may be able to interact with T cells in the B cell area. Finally, $CXCR5^+$ DCs may receive additional conditioning signals from the nearby B cells, FDCs or MRCs, that will direct the DCs to induce IL-4 and Bcl6 expression in the responding T cells. Each of these possibilities will need to be addressed.

Collectively, our results support a model of DC-driven $CD4^+$ T cell differentiation in which pathogen-derived signals instruct DCs to upregulate CXCR5, migrate to a unique microenvironment in the LN and initiate T_{FH} and T_H2 development. Although we do not know whether this model is applicable to all T_H2 responses, we recently found that T_H2 responses in *Leishmania major*-infected BALB/c mice are controlled in a similar CXCR5 and CXCL13-dependent fashion (B. Leon and F. Lund, unpublished). Finally, and perhaps most importantly, our data suggest that some T_H2 responses may be attenuated with therapeutics that deplete B cells or block CXCL13 or LT signaling.

Methods

Mice and infections

All animals were bred within the University of Rochester Animal Facilities and all procedures were approved by the the University of Rochester Animal Care and Use Committee. C57BL/6J (B6), B6.SJL-*Ptprc*^{a}*Pepc*^{b}/BoyJ ($CD45.1^+$ B6 congenics), B6.129S2-*Ighm*^{tm1Cgn}/J (μMT), B6.FVB-Tg(Itgax-DTR/EGFP)57Lan/J (CD11c-DTR), B6.129X1-Cxcl13^{tm1Cys}/J (*Cxcl13*$^{-/-}$), B6.129S2(Cg)-Cxcr5^{tm1Lipp}/J (*Cxcr5*$^{-/-}$), C57BL/6J-Lta^{hlb382}/J (*Lta*$^{-/-}$) were originally obtained from Jackson laboratory. B6.129-Il4^{tm1Lky}/J (B6 4get IL-4 reporter mice) and B6.129-Il4^{tm1Lky}/J.IgHm^{tm1Cgn}/J (4getμMT), were obtained from M. Mohrs (Trudeau Institute), C57BL/6-Tg(IghelMD4)4Ccg/J.IgHm^{tm1Cgn}/J (MD4μMT) mice were obtained from J. Kearney (Univ. Alabama-Birmingham) and B6N.DDD-plt/NknoJ (*plt/plt*) mice were obtained from J. Cyster (Univ. California-San Francisco). Adult mice were infected by gavage with 200 L3 *Hp* larvae or intranasally with 0.1 LD_{50} of influenza H3N2 A/X31.

BM chimeras

Recipient mice were irradiated with 950 Rads from a ^{137}Cs source delivered in a split dose and reconstituted with 10^7 total BM cells. To generate CD11c-DTR BM chimeras B6 recipients were reconstituted with 100% CD11c-DTR BM. To generate DC-*Cxcr5*$^{-/-}$ and DC-WT chimeras, B6 recipients were reconstituted with either 80% CD11c-DTR BM + 20% *Cxcr5*$^{-/-}$ BM or 80% CD11c-DTR BM + 20% B6 BM. To generate B-*Lta*$^{-/-}$ and B-WT chimeras, μMT recipients were reconstituted with 80% μMT BM + 20% *Lta*$^{-/-}$ BM or 80% μMT BM + 20% B6 BM. To generate B6:*Cxcr5*$^{-/-}$ 50:50 mixed BM chimeras, $CD45.1^+$ B6 congenic recipients were reconstituted with 50% $CD45.1^+$ B6 BM and 50% *Cxcr5*$^{-/-}$ BM. Experiments were initiated with the chimeric mice 8–12 weeks post-reconstitution.

In vivo depletion and blocking studies

To block LTβR signaling *in vivo*, mice were treated i.p. at the time of infection, with 100 μg of either LTβR-Ig fusion protein[43] (Biogen Idec) or control human Ig protein. To block *in vivo* CXCL13 activity, mice were injected (i.p.) at the time of infection with either 200 μg anti-mouse CXCL13 (clone 43614, R&D Systems) or isotype control antibody. To deplete $CD20^+$ B cells, mice were injected i.p. 4 days before infection with 250 μg of mouse anti-mouse CD20 (ref. 44) (clone 18B12, IgG2a isotype, Biogen Idec) or isotype control antibody (clone 2B8). To deplete $CD11c^+$ cells *in vivo*, CD11c-DTR BM chimeras were treated with 60 ng DT (Sigma-Aldrich) and then immediately infected. Mice received additional injections of DT on day 3 and 5.

Cell preparation and flow cytometry

Cells, isolated from the LNs, spleen or peritoneal cavity were pre-incubated with anti-mouse CD16/32 (5 μg/ml; clone 2.4G2, BD-Biosciences) and then stained with fluorochrome-conjugated Abs. Conjugated antibodies to CD205 (NLDC-145), CD11c (HL3), B220 (RA3-6B2), CD19 (1D3), CD40 (3/23), MHCII (AF6-120.1), CD4 (GK1.5), CD44 (IM7), CCR7 (4B12), CXCR5 (2G8), PD-1 (J43), ICOS (7E.17G9), CD45.1(A20) and CD45.2 (104) were purchased from from Cedarlane Laboratories (CD205) or BD-Biosciences (all others). The I-A(b)class II tetramers containing $NP_{311–325}$ peptide were generated by NIH Tetramer Core Facility (Atlanta, GA). For intracellular staining, LN single-cell suspensions were stimulated on anti-CD3-coated plates (2 μg/ml) in the presence of Brefeldin-A (BFA, 10 μg/ml) for 4 h. Restimulated cells were surface stained, fixed in 4% paraformaldehyde, permeabilized with 0.1% saponin, and stained with Abs against IL-4 (BVD4-1D11), IL-13 (13A) or IFN-γ (XMG1.2) (BD-Biosciences). Bcl6 (clone K112-91, BD-Biosciences) intracellular staining was performed using the Mouse regulatory T cell staining kit (eBioscience). To detect LT, cells were stained with LTβR-Ig or human Ig control protein, followed by conjugated Fab'2 anti-human IgG, mouse absorbed Abs (Southern Biotechnology Associates, Inc.). In some experiments cells were preincubated with unconjugated anti-LTβ antibody (BBF6; Biogen Idec) to inhibit LTβR-binding to LT. Cells were analyzed using FACSCanto II (BD-Biosciences) and C6 (Accuri) Flow Cytometers located in the University of Rochester Flow Cytometry Core Facility.

Cell purifications, T cell transfers and *in vitro* cultures

DCs from pooled LNs were purified on LS columns using anti-CD11c MACs beads (Miltenyi Biotec) and then stained with fluorochrome-labeled Abs to MHCII (AF6-120.1), B220 (RA3-6B2) and CD11c (HL3). DC subsets were purified using a FACSAria sorter in the Univ. of Rochester Flow Cytometry Core. $CD4^+$ T cells were isolated by MACs from the spleens of naïve $CD45.1^+$ B6 congenics or from the mesLNs of *Hp*-infected IL-4 reporter mice (day 5 post-infection). All T cell preparations were more than 95% pure. $CD45.1^+$ B6 naïve T cells (1×10^7/mouse) were injected (i.v.) into BM chimeric mice that were subsequently infected with *Hp*. 2×10^4 DCs and 1×10^5 $CD4^+$ T cells purified from mesLNs of *Hp*-infected or uninfected mice were co-cultured in round-bottomed 96-well plates for 96 h at 37°C in 200 μl of complete medium containing RPMI 1640m sodium

pyruvate, HEPES (pH 7.4), non-essential amino acids, penicillin, streptomycin, 2-mercaptoethanol and 10% heat-inactivated FBS (Gibco).

Migration assays

CXCL13 (1 μg/ml) or CCL19 (0.1 μg/ml) in RPMI-1% FBS (R&D Systems) was added to the bottom chamber of 24-well transwell plates (polycarbonate filter with 5 μm pore, Costar). DCs or B cells (1×10^5 cells/transwell) were added to the upper chamber and incubated at 37°C for 90 min. Transmigrated cells were collected from the lower chamber, stained and counted on a flow cytometer, using Accuri C6 CFlow software. Results are represented as the mean ± SD of the chemotaxis index (CI) or as the percentage of input cells that migrated in the assay. The CI represents the fold increase in the number of migrated cells in response to chemoattractants over the spontaneous cell migration (to control medium).

Immunofluorescence

Frozen sections (5 μm), prepared from OCT (Sakura Finetek) embedded LNs,, were incubated with 10 μg/ml of Fc block and 5% normal donkey serum in PBS and then stained with FITC-labeled anti-CD11c (HL3), biotin-labeled anti-CD4 (L3T4), biotin-labeled anti-CD8α (53-6.7) or Alexa Fluor 648-labeled anti-B220 (RA3-6B2). Primary antibodies were detected with Alexa Fluor 488 labeled goat anti-FITC and streptavidin–Alexa Fluor 555 (Invitrogen Life Sciences). Slides were mounted with Slow Fade Gold Antifade (Invitrogen). Images were collected with a Zeiss Axioplan 2 microscope and recorded with a Zeiss Axiocam digital camera (Zeiss). The images were taken with a 20x objective for 200x final magnification. Images were collected using Zeiss Axiovision Image software and saved as JPEG files.

Real-time PCR

2 μg of DNase-treated RNA, extracted from mesLNs (RNeasy, QIAGEN), was reverse transcribed with random hexamers and Superscript II (Invitrogen). Quantitative PCR was performed using Taqman master mix and primers and probes for *Cxcl13* (Applied Biosystems). All reactions were run on a Lightcycler 480 Real-time PCR System (Roche). *Clxc13* mRNA abundance was determined and then normalized to *Gapdh* mRNA abundance. Data are reported as the fold-change in expression relative to mesLN cells from *Hp*-infected control mice. The data are represented as the average of three independent samples.

Statistical Analyses

GraphPad Prism software (Version 5.0a) was used for data analysis. Data were analyzed using the unpaired Student's *t* test. Values of $P \leq 0.05$ were considered significant.

Supplementary Material

Refer to Web version on PubMed Central for supplementary material.

Acknowledgments

The authors thank L. LaMere (Univ. Rochester), A. Bucher (Univ. Rochester) and K. Martin (Univ. Rochester) for management of animal breeding and genotyping and acknowledge the University of Rochester Flow Facility Core for cell sorting and the NIH tetramer facility for providing the flu NP-specific CD4 tetramers. The authors also thank M. Mohrs (Trudeau Institute), J. Kearney (Univ. Alabama-Birmingham) and J. Cyster (Univ. California-San Francisco) for providing mouse strains used in this manuscript. This work was supported by the University of Rochester and National Institutes of Health grants NIAID AI068056 and AI078907 to F.E. Lund and NIAID AI061511 to T.D. Randall.

References

1. Cyster JG. Leukocyte migration: scent of the T zone. Curr Biol. 2000; 10:R30–33. [PubMed: 10660291]
2. Forster R, Davalos-Misslitz AC, Rot A. CCR7 and its ligands: balancing immunity and tolerance. Nat Rev Immunol. 2008; 8:362–371. [PubMed: 18379575]
3. Gunn MD, et al. Mice lacking expression of secondary lymphoid organ chemokine have defects in lymphocyte homing and dendritic cell localization. J Exp Med. 1999; 189:451–460. [PubMed: 9927507]
4. Mori S, et al. Mice lacking expression of the chemokines CCL21-ser and CCL19 (plt mice) demonstrate delayed but enhanced T cell immune responses. J Exp Med. 2001; 193:207–218. [PubMed: 11148224]
5. Nakano H, et al. Blood-derived inflammatory dendritic cells in lymph nodes stimulate acute T helper type 1 immune responses. Nat Immunol. 2009; 10:394–402. [PubMed: 19252492]
6. Schaerli P, et al. CXC chemokine receptor 5 expression defines follicular homing T cells with B cell helper function. J Exp Med. 2000; 192:1553–1562. [PubMed: 11104798]
7. Vinuesa CG, Cyster JG. How T cells earn the follicular rite of passage. Immunity. 2011; 35:671–680. [PubMed: 22118524]
8. Crotty S. Follicular helper CD4 T cells (TFH). Annu Rev Immunol. 2011; 29:621–663. [PubMed: 21314428]
9. Yu P, et al. B cells control the migration of a subset of dendritic cells into B cell follicles via CXC chemokine ligand 13 in a lymphotoxin-dependent fashion. J Immunol. 2002; 168:5117–5123. [PubMed: 11994465]
10. Saeki H, Wu MT, Olasz E, Hwang ST. A migratory population of skin-derived dendritic cells expresses CXCR5, responds to B lymphocyte chemoattractant in vitro, and co-localizes to B cell zones in lymph nodes in vivo. Eur J Immunol. 2000; 30:2808–2814. [PubMed: 11069061]
11. Cyster JG, et al. Follicular stromal cells and lymphocyte homing to follicles. Immunol Rev. 2000; 176:181–193. [PubMed: 11043777]
12. Tew JG, Wu J, Fakher M, Szakal AK, Qin D. Follicular dendritic cells: beyond the necessity of T-cell help. Trends Immunol. 2001; 22:361–367. [PubMed: 11429319]
13. Katakai T, et al. Organizer-like reticular stromal cell layer common to adult secondary lymphoid organs. J Immunol. 2008; 181:6189–6200. [PubMed: 18941209]
14. Choi YS, et al. ICOS receptor instructs T follicular helper cell versus effector cell differentiation via induction of the transcriptional repressor Bcl6. Immunity. 2011; 34:932–946. [PubMed: 21636296]
15. Baumjohann D, Okada T, Ansel KM. Cutting Edge: Distinct waves of BCL6 expression during T follicular helper cell development. J Immunol. 2011; 187:2089–2092. [PubMed: 21804014]
16. Goenka R, et al. Cutting edge: dendritic cell-restricted antigen presentation initiates the follicular helper T cell program but cannot complete ultimate effector differentiation. J Immunol. 2011; 187:1091–1095. [PubMed: 21715693]
17. MartIn-Fontecha A, et al. Regulation of dendritic cell migration to the draining lymph node: impact on T lymphocyte traffic and priming. J Exp Med. 2003; 198:615–621. [PubMed: 12925677]

18. Sallusto F, Lanzavecchia A. Understanding dendritic cell and T-lymphocyte traffic through the analysis of chemokine receptor expression. Immunol Rev. 2000; 177:134–140. [PubMed: 11138771]
19. Ballesteros-Tato A, Leon B, Lund FE, Randall TD. Temporal changes in dendritic cell subsets, cross-priming and costimulation via CD70 control CD8(+) T cell responses to influenza. Nat Immunol. 2010; 11:216–224. [PubMed: 20098442]
20. Mohrs M, Shinkai K, Mohrs K, Locksley RM. Analysis of type 2 immunity in vivo with a bicistronic IL-4 reporter. Immunity. 2001; 15:303–311. [PubMed: 11520464]
21. Ansel KM, et al. A chemokine-driven positive feedback loop organizes lymphoid follicles. Nature. 2000; 406:309–314. [PubMed: 10917533]
22. Forster R, et al. A putative chemokine receptor, BLR1, directs B cell migration to defined lymphoid organs and specific anatomic compartments of the spleen. Cell. 1996; 87:1037–1047. [PubMed: 8978608]
23. Jung S, et al. In vivo depletion of CD11c+ dendritic cells abrogates priming of CD8+ T cells by exogenous cell-associated antigens. Immunity. 2002; 17:211–220. [PubMed: 12196292]
24. Ngo VN, et al. Lymphotoxin alpha/beta and tumor necrosis factor are required for stromal cell expression of homing chemokines in B and T cell areas of the spleen. J Exp Med. 1999; 189:403–412. [PubMed: 9892622]
25. De Togni P, et al. Abnormal development of peripheral lymphoid organs in mice deficient in lymphotoxin. Science. 1994; 264:703–707. [PubMed: 8171322]
26. Steinman RM, Pack M, Inaba K. Dendritic cells in the T-cell areas of lymphoid organs. Immunol Rev. 1997; 156:25–37. [PubMed: 9176697]
27. Jenkins MK, et al. In vivo activation of antigen-specific CD4 T cells. Annu Rev Immunol. 2001; 19:23–45. [PubMed: 11244029]
28. Paul WE, Zhu J. How are T(H)2-type immune responses initiated and amplified? Nat Rev Immunol. 2010; 10:225–235. [PubMed: 20336151]
29. Zaretsky AG, et al. T follicular helper cells differentiate from Th2 cells in response to helminth antigens. J Exp Med. 2009; 206:991–999. [PubMed: 19380637]
30. Nakayamada S, et al. Early Th1 cell differentiation is marked by a Tfh cell-like transition. Immunity. 2011; 35:919–931. [PubMed: 22195747]
31. King IL, Mohrs M. IL-4-producing CD4+ T cells in reactive lymph nodes during helminth infection are T follicular helper cells. J Exp Med. 2009; 206:1001–1007. [PubMed: 19380638]
32. Wojciechowski W, et al. Cytokine-producing effector B cells regulate type 2 immunity to H. polygyrus. Immunity. 2009; 30:421–433. [PubMed: 19249230]
33. Liu Q, et al. The role of B cells in the development of CD4 effector T cells during a polarized Th2 immune response. J Immunol. 2007; 179:3821–3830. [PubMed: 17785819]
34. Crawford A, Macleod M, Schumacher T, Corlett L, Gray D. Primary T cell expansion and differentiation in vivo requires antigen presentation by B cells. J Immunol. 2006; 176:3498–3506. [PubMed: 16517718]
35. Linton PJ, et al. Costimulation via OX40L expressed by B cells is sufficient to determine the extent of primary CD4 cell expansion and Th2 cytokine secretion in vivo. J Exp Med. 2003; 197:875–883. [PubMed: 12668647]
36. Fu YX, Huang G, Wang Y, Chaplin DD. B lymphocytes induce the formation of follicular dendritic cell clusters in a lymphotoxin alpha-dependent fashion. J Exp Med. 1998; 187:1009–1018. [PubMed: 9529317]
37. Gonzalez M, Mackay F, Browning JL, Kosco-Vilbois MH, Noelle RJ. The sequential role of lymphotoxin and B cells in the development of splenic follicles. J Exp Med. 1998; 187:997–1007. [PubMed: 9529316]
38. Endres R, et al. Mature follicular dendritic cell networks depend on expression of lymphotoxin beta receptor by radioresistant stromal cells and of lymphotoxin beta and tumor necrosis factor by B cells. J Exp Med. 1999; 189:159–168. [PubMed: 9874572]
39. Ngo VN, Cornall RJ, Cyster JG. Splenic T zone development is B cell dependent. J Exp Med. 2001; 194:1649–1660. [PubMed: 11733579]

40. Junt T, et al. Subcapsular sinus macrophages in lymph nodes clear lymph-borne viruses and present them to antiviral B cells. Nature. 2007; 450:110–114. [PubMed: 17934446]
41. Phan TG, Grigorova I, Okada T, Cyster JG. Subcapsular encounter and complement-dependent transport of immune complexes by lymph node B cells. Nat Immunol. 2007; 8:992–1000. [PubMed: 17660822]
42. Matsuura J, Sakanaka M, Sato N, Ichikawa A, Tanaka S. Suppression of CXCR4 expression in mast cells upon IgE-mediated antigen stimulation. Inflamm Res. 2010; 59:123–127. [PubMed: 19696965]
43. Fava RA, et al. A role for the lymphotoxin/LIGHT axis in the pathogenesis of murine collagen-induced arthritis. J Immunol. 2003; 171:115–126. [PubMed: 12816989]
44. Hamel K, et al. Suppression of proteoglycan-induced arthritis by anti-CD20 B Cell depletion therapy is mediated by reduction in autoantibodies and CD4+ T cell reactivity. J Immunol. 2008; 180:4994–5003. [PubMed: 18354225]

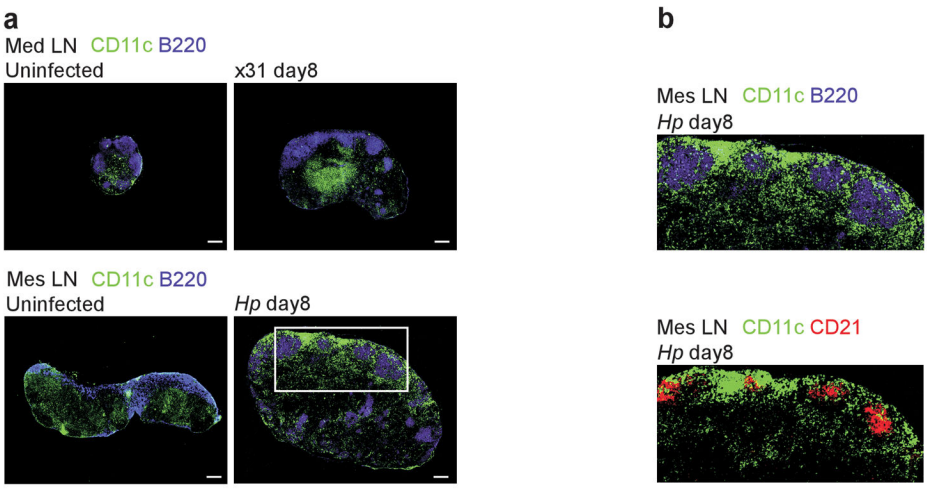

Figure 1. DCs migrate to the peri- and interfollicular areas of LNs following *Hp* infection

(**a,b**) B6 mice were infected by gavage with 200 L3 *Hp* or intranasally with 0.1 LD_{50} of x31 influenza virus. Cryosections from the medLNs or mesLNs of uninfected or day 8 infected mice were stained anti-CD11c, anti-B220 and anti-CD21. The region within the box in panel (**a**) was enlarged in panel (**b**). Scale bar = 400 μm. All data are representative of three or more independent experiments.

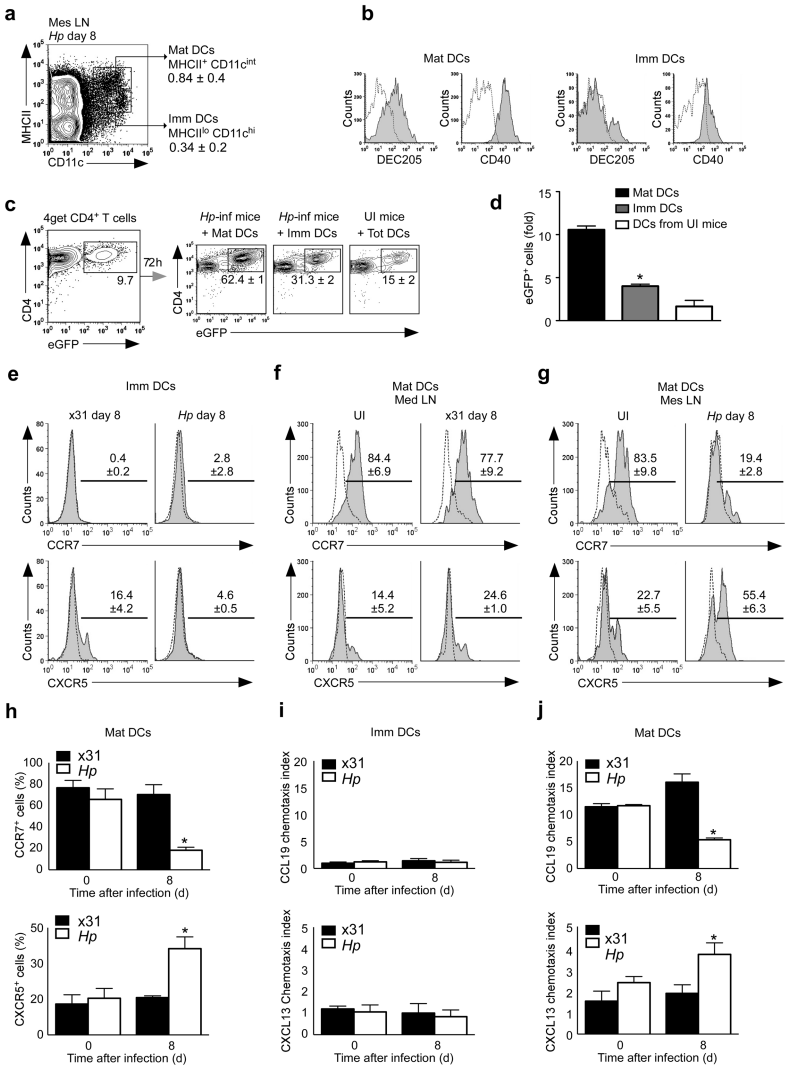

Figure 2. *Hp* antigen-bearing mature DCs express CXCR5 and display increased responsiveness to CXCL13 and reduced responsiveness to CCL19

(**a,b**) mesLN cells from day 8 *Hp*-infected B6 mice were analyzed by flow cytometry. Gated mature (mat) MHCII^{+}CD11c^{int} and immature (imm) MHCII^{lo}CD11c^{hi} DCs (**a**) were analyzed for expression of DEC205 and CD40 ((**b**), filled histograms). Open histograms represent non-specific control staining. (**c,d**) CD4^{+} T cells from mesLNs of day 5 *Hp*-infected IL-4 reporter (4get) mice were purified and co-cultured with total DCs (tot DCs) purified from uninfected (UI) mice or with sort-purified mature (MHCII^{+}CD40^{hi}CD11c^{int} DCs) and immature (MHCII^{lo}CD40^{lo}CD11c^{hi}) DCs isolated from the mesLNs of day 8 *Hp*-infected mice. The population expansion (**c**) of IL-4 mRNA-expressing (EGFP^{+}) CD4^{+} T cells was measured at 72 h and the fold increase (**d**) in EGFP^{+} CD4^{+} T cells was determined (mean ± SD n = 5). (**e–h**) MHCII^{lo}CD40^{lo}CD11c^{hi} immature (**e**) and MHCII^{+}CD40^{hi}CD11c^{int} mature (**f–h**) DCs from day 8 x31-infected mice (**e,f**), day 8 *Hp*-infected mice (**e,g**) and uninfected mice (**f–h**) were analyzed by flow cytometry for expression of CCR7 and CXCR5. The frequency of positive cells is shown as the Mean ± SD (n = 4–5). (**i,j**) MHCII^{lo}CD40^{lo}CD11c^{hi} immature (**i**) and MHCII^{+}CD40^{hi}CD11c^{int}

mature (**j**) DCs from x31-infected and *Hp*-infected mice were analyzed in transwell chemotaxis assays using CCL19 or CXCL13 as chemoattractants. Data are expressed as the mean ± SD (**n** = 3) of the chemotaxis index (CI). The data are representative of at least three independent experiments. (*P<0.001)

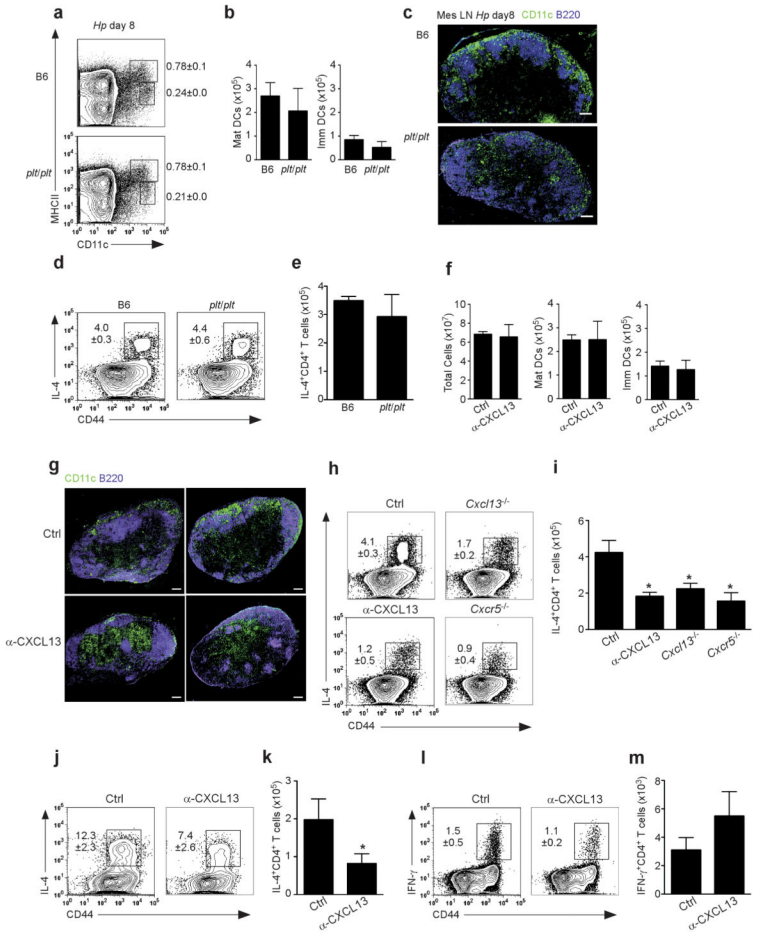

Figure 3. CXCL13, but not CCL19 or CCL21a, control DC positioning in the LN and Th2 development following *Hp* infection

(**a–e**) B6 and *plt/plt* mice were infected with *Hp* and analyzed on day 8. The frequencies (**a**) and numbers (**b**) of MHCII^{lo}CD11c^{hi} immature DCs and MHCII^{+}CD11c^{int} mature DCs in the mesLNs were determined. (**c**) Cryosections of mesLNs from *Hp*-infected mice were stained with anti-CD11c and anti-B220. Scale bar = 400 μm. (**d–e**) mesLN cells from *Hp*-infected *plt/plt* or B6 mice were restimulated with anti-CD3 + BFA for 4 h. The frequencies (**d**) and numbers (**e**) of IL-4-producing CD4^{+} T cells were determined by ICCS. (**f–m**) B6 mice were treated with 200 μg anti-CXCL13 or control antibody at the time of infection with *Hp* (**f–k**) or influenza x31 (**l–m**). Analyses were performed 8 days post-infection. (**f**) The numbers of total cells, MHCII^{lo}CD11c^{hi} immature DCs and MHCII^{+}CD11c^{int} mature DCs in the mesLNs of *Hp*-infected mice were determined using flow cytometry. (**g**) Cryosections of mesLNs from *Hp*-infected mice were stained with anti-CD11c and anti-B220. Scale bar = 400 μm. (**h–k**) Cells from *Hp*-infected *Cxcl13*$^{-/-}$ or *Cxcr5*$^{-/-}$ mice or anti-CXCL13-treated or control-treated B6 mice were restimulated with anti-CD3 + BFA for 4 h. The frequencies (**h,j**) and numbers (**i,k**) of IL-4-producing CD4^{+} T cells present in the mesLN (**h–i**) and PEC (**j,k**) were determined by ICCS. (**l,m**) Cells from the medLN of influenza-infected anti-CXCL13 or control-treated B6 mice were restimulated with anti-CD3 + BFA for 4 h. The frequencies (**l**) and numbers (**m**) of IFN-γ-producing CD4 T cells were determined by ICCS.

Data are representative of two or more independent experiments (mean ± SD of five mice per group, *P<0.01 vs control).

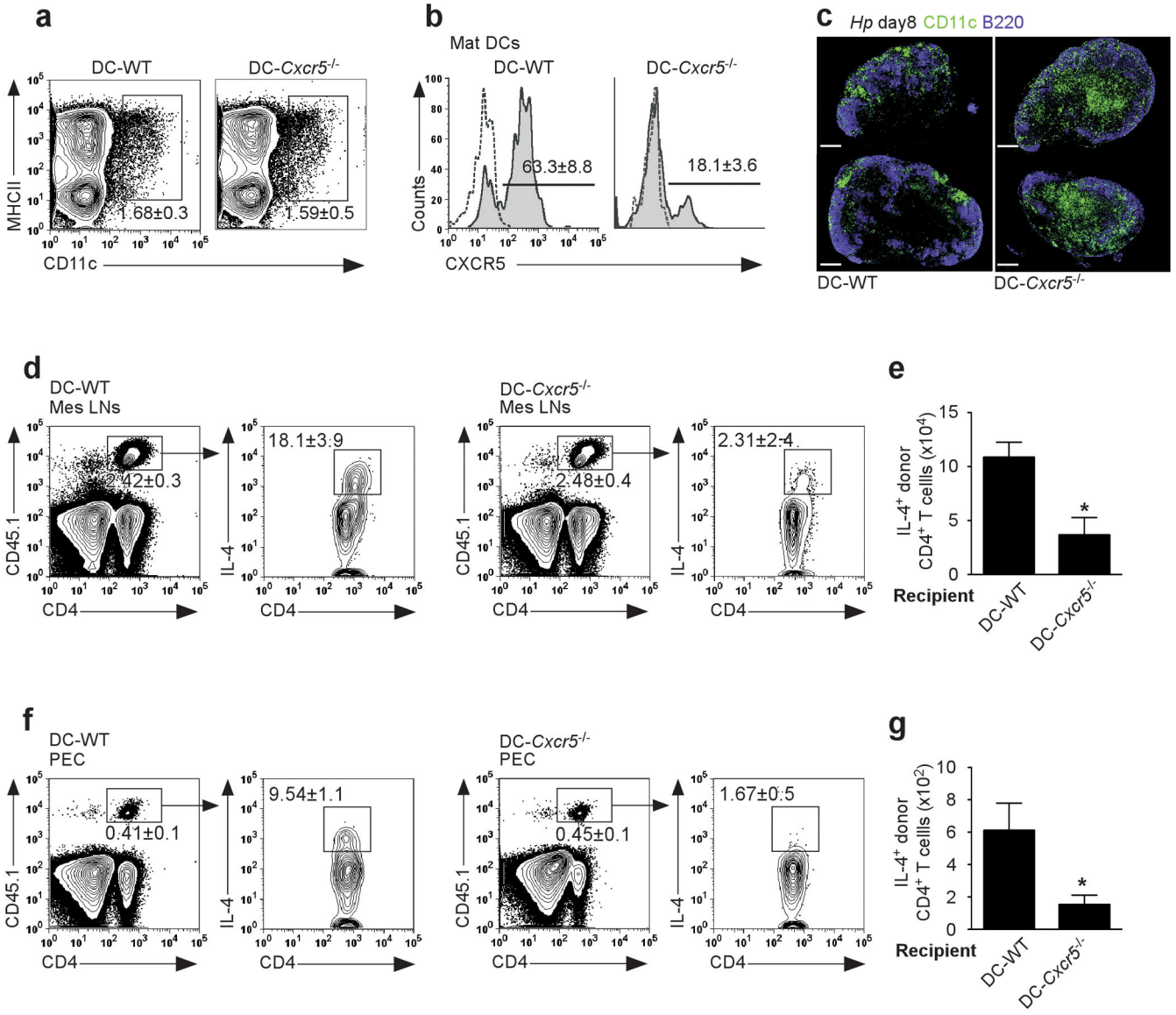

Figure 4. Development of IL-4 producing T cells following *Hp* infection is controlled by CXCR5-expressing DCs

(**a–g**). DC-WT and DC-*Cxcr5*$^{-/-}$ chimeras were infected with *Hp*, treated with DT on days 0, 3 and 5 post-infection and analyzed on day 8. **(a,b)** The frequencies of total DCs (**a**) and CXCR5-expressing MHCII^{+}CD11c^{int} mature DCs (**b**) are shown. (**c**) Cryosections from mesLNs of infected chimeras were stained with anti-CD11c and anti-B220. Scale bar = 400 μm (**d–g**). mesLN (**d,e**) and PEC (**f,g**) cells from infected chimeras were restimulated with plate-bound anti-CD3 + BFA for 4 h. The frequencies (**d,f**) and numbers (**e,g**) of IL-4^{+} donor wild-type CD45.1^{+} CD4 T cells in each tissue were determined by flow cytometry. Data are representative of two or more independent experiments (mean ± SD of five mice per group, *P<0.001).

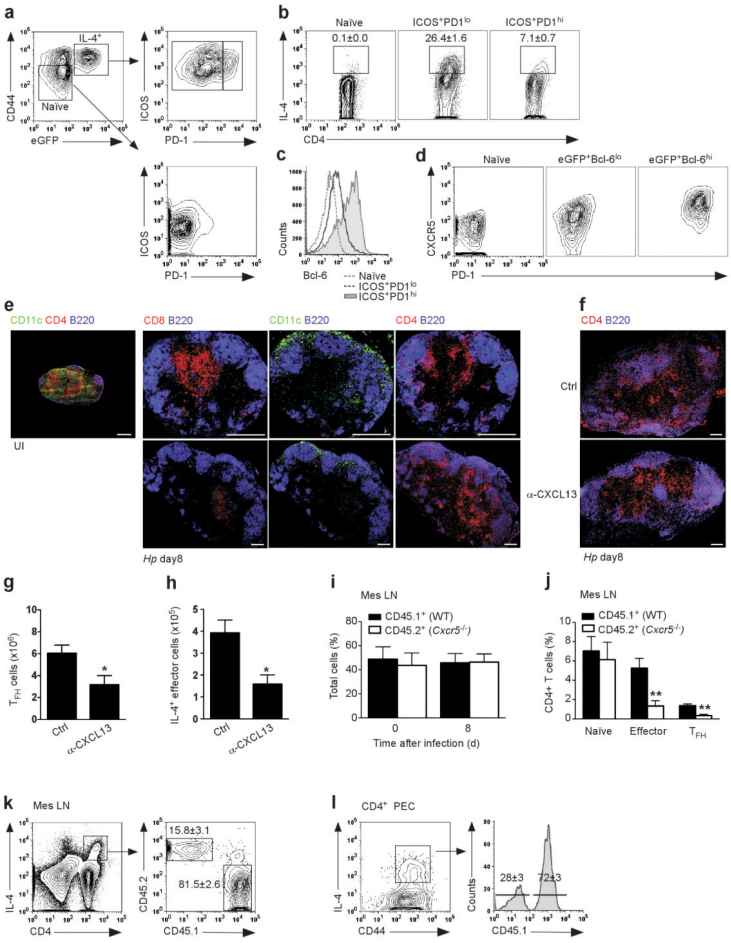

Figure 5. CXCR5 is expressed by LN T_{FH} and T_H2 cells and is required for T_{FH} and Th2 cell development following *Hp* infection

(**a–d**) mesLN cells from day 8 *Hp*-infected IL-4 (EGFP) reporter mice were analyzed by flow cytometry. (**a**) $CD4^+$ T cells were divided into naïve ($CD44^{lo}EGFP^-$) and antigen-experienced ($CD44^{hi}EGFP^+$) populations, analyzed for expression of ICOS and PD-1 and subdivided into naïve ($CD44^{lo}EGFP^-ICOS^-PD\text{-}1^-$), T_{FH} ($CD44^{hi}EGFP^+ICOS^+PD\text{-}1^{hi}$) and T effector ($CD44^{hi}EGFP^+ICOS^+PD\text{-}1^{lo}$) subsets. (**b**) mesLN cells were restimulated with anti-CD3 + BFA for 4 h and the frequencies of IL-4^+ naïve, $ICOS^+PD\text{-}1^{lo}$ and $ICOS^+PD\text{-}1^{hi}$ CD4 T cells were determined by ICCS. (**c,d**) Intracellular staining to detect Bcl6 was performed on non-restimulated mesLN cells. Bcl6 expression in naïve, $ICOS^+PD\text{-}1^{lo}$ and $ICOS^+PD\text{-}1^{hi}$ gated CD4 T cells is shown in (**c**) and CXCR5 and PD-1 expression on gated naïve, $EGFP^+Bcl6^{lo}$ and $EGFP^+Bcl6^{hi}$ $CD4^+$ T cells are shown in panel **d** (see also gating strategy in Supplementary Fig. 5d). (**e**) Serial cryosections of mesLNs from uninfected or day 8 *Hp*-infected B6 mice were stained with anti-CD8, anti-B220, anti-CD11c or anti-CD4 (Scale bar = 400 μm). (**f–h**) B6 mice were treated with anti-CXCL13 or control antibody, infected with *Hp* and analyzed on day 8. Cryosections (**f**) of mesLNs were stained with anti-CD4 and anti-B220 (Scale bar = 400 μm). mesLN cells were analyzed by flow cytometry immediately *ex vivo* (**g**) or following 4 h restimulation with anti-CD3 + BFA (**h**). The numbers of $ICOS^+PD\text{-}1^{hi}CD44^{hi}$ T_{FH} cells (**g**) and IL-$4^+ICOS^+PD\text{-}1^{lo}$ T_H2 cells (**h**) are

shown. (**i–l**) Chimeric mice reconstituted with 50% CD45.1$^+$ B6 BM and 50% CD45.2$^+$ *Cxcr5*$^{-/-}$ BM were infected with *Hp* and analyzed on day 8 post-infection. (**j**) The frequencies of total CD45.1$^+$ and CD45.2$^+$ cells in the mesLN and within the gated naïve (CD44^{lo}), ICOS$^+$PD-1^{hi} T_{FH} and ICOS$^+$PD-1^{lo} effector CD4 populations were determined by flow cytometry. (**k,l**) The mesLN cells were restimulated with anti-CD3 + BFA for 4 h and the frequencies of CD45.1$^+$ and CD45.2$^+$ cells within the gated IL-4$^+$ CD4 T cell population were determined in the mesLN (**k**) and PEC (**l**) by ICCS. Data are representative of three independent experiments (mean ± SD of five mice per group, *P<0.01, **P<0.001).

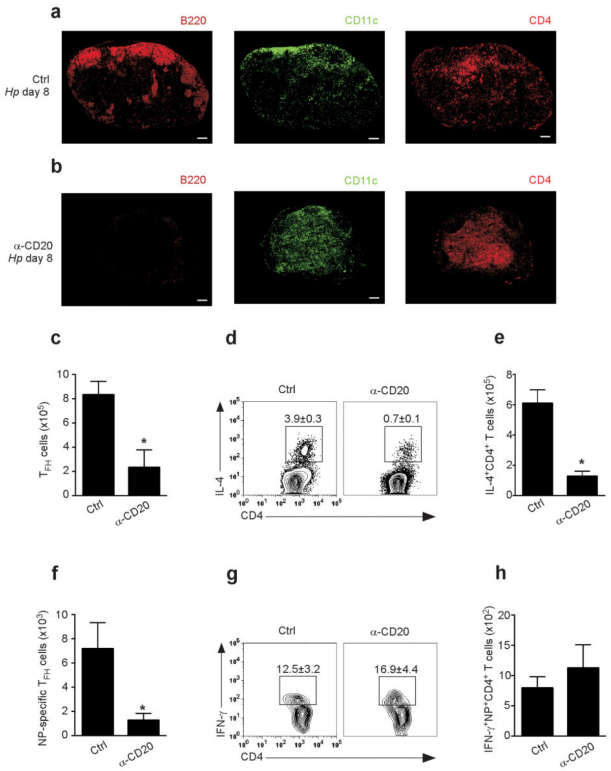

Figure 6. B cells depletion alters the site of co-localization between DCs and CD4 T cells in the LN and prevents the development of T_{FH} and T_H2 cells, but not T_H1 cells

(**a–h**) B6 mice were treated with 250 μg of anti-CD20 or control antibody 4 days before infection with either *Hp* (**a–e**) or influenza x31 (**f–h**). Analyses were performed on day 8 post-infection. (**a,b**) Cryosections of mesLNs from *Hp*-infected control-treated (**a**) or anti-CD20 treated (**b**) mice were stained with anti-B220, anti-CD11c, and anti-CD4. Scale bar = 400 μm. (**c–e**) Cells from *Hp*-infected mesLNs were analyzed by flow cytometry either *ex vivo* (**c**) or following 4 h restimulation with anti-CD3 + BFA (**d,e**). The numbers of $ICOS^+PD\text{-}1^{hi}$ T_{FH} cells (**c**) and the frequencies (**d**) and numbers (**e**) of IL-4^+ $ICOS^+PD\text{-}1^{lo}$ $CD4^+$ T cells are shown. (**f–h**) NP^+ (influenza-specific) $CD4^+$ T cells from medLN of influenza-infected anti-CD20 or control treated mice were analyzed by flow cytometry either *ex vivo* (**f**) or following 4 h restimulation with anti-CD3 + BFA (**g,h**). The numbers of flu-specific $NP^+ICOS^+PD\text{-}1^{hi}$ T_{FH} cells (**f**) and the frequencies (**g**) and numbers (**h**) of IFN-γ-producing $NP^+ICOS^+PD\text{-}1^{lo}$ $CD4^+$ T cells are shown (mean ± SD of five mice per group, *P<0.001). Data are representative of three independent experiments.

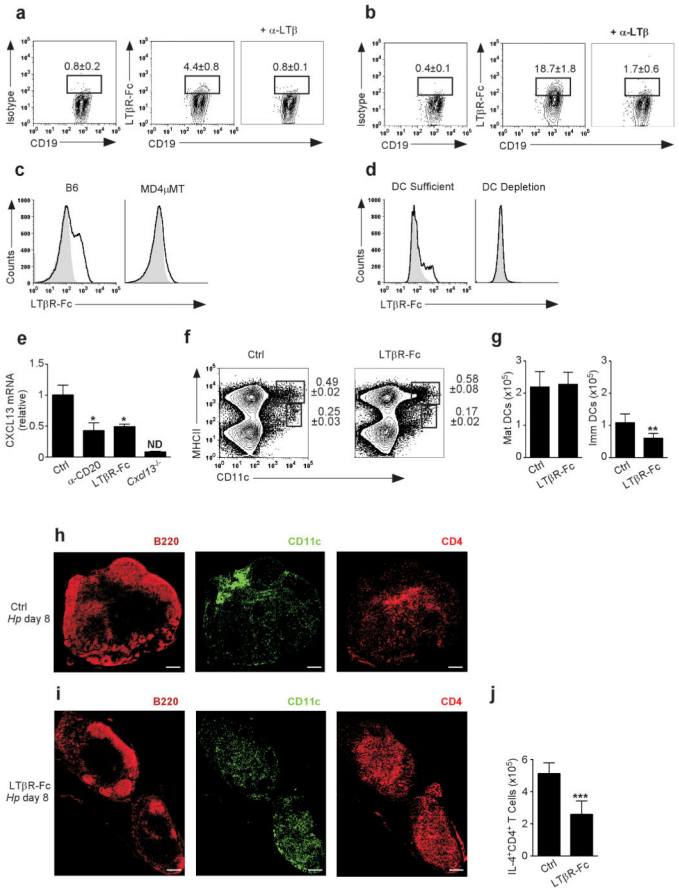

Figure 7. LT blockade downregulates CXCL13 expression, prevents co-localization of DCs and T cells within the B cell area and impairs T_H2 development in LNs of *Hp*-infected mice

(**a,b**) Membrane LT expression on mesLN cells from naïve (**a**) and day 8 *Hp*-infected B6 mice (**b**) were were determined by flow cytometry. Control staining in the presence of anti-LTβ blocking antibody is shown. (**c**) $CD19^+$ B cells from day 8 *Hp*-infected B6 and MD4μMT mice were stained with mLTβR-Fc (open histograms) or control antibody (filled histogram). (**d**) CD11c-DTR BM chimeric mice, treated with PBS (DC sufficient) or DT on days 0 and 3 (DC depletion), were infected with *Hp*. LT expression (open histogram) is shown on $CD19^+$ B cells. Isotype control staining is shown in filled histogram. (**e–j**) B6 mice were treated (i.p.) with 100 μg of LTβR-Fc fusion protein or control protein at the time of *Hp* infection or with 250 μg of anti-CD20 or control Ab four days before *Hp* infection. Analyses were performed on day 8 post-infection. (**e**) Cxcl13 mRNA in mesLN cells were determined by quantitative PCR. Data show mean ± SD of three samples. nd=not detected. (**f,g**) The frequencies (**f**) and numbers (**g**) of $MHCII^+CD11c^{int}$ mature and $MHCII^{lo}CD11c^{hi}$ immature mesLN DCs in LTβR-Fc and control-treated B6 mice were determined by flow cytometry. (**h,i**) Cryosections from mesLNs of control (**h**) and LTβR-Fc treated mice (**i**) were stained with anti-B220, anti-CD11c and anti-CD4. Scale bar = 400 μm. (**j**) mesLN cells were restimulated with anti-CD3 + BFA for 4 h and the numbers of IL-4^+ $CD4^+$ T cells from LTβR-Fc-treated mice and B6 controls were determined by ICCS. Data are representative of three independent experiments (mean ± SD of five mice per group, *P<0.001 vs control, **P<0.05, ***P<0.01).

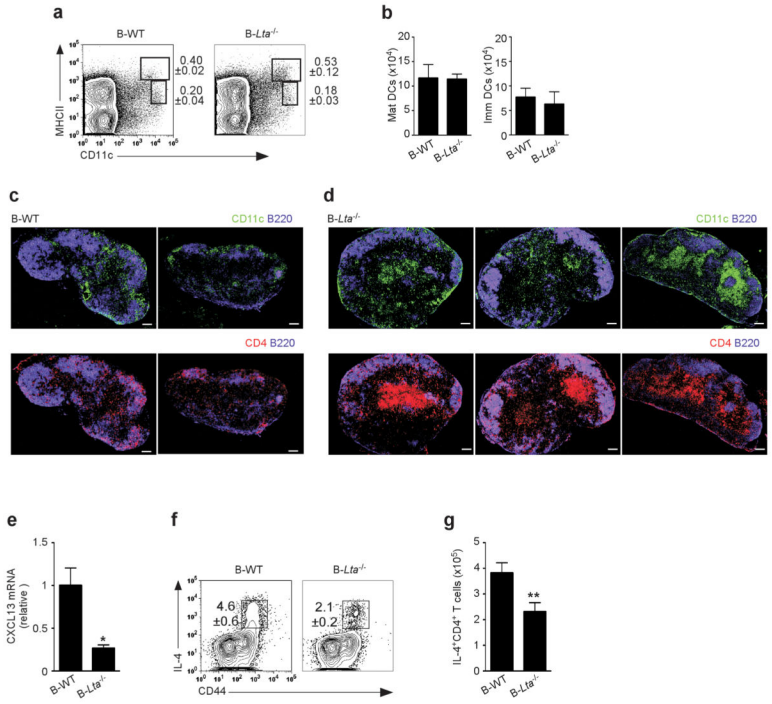

Figure 8. B cell-derived LT facilitates DC migration to the B cell area of LNs following *Hp* infection and modulates T_H2 development

(**a–g**) B-WT and B-*Lta*$^{-/-}$ chimeras were infected with *Hp* and analyzed on day 8 post-infection. (**a,b**) The frequencies (**a**) and numbers (**b**) of MHCII^{+}CD11c^{int} mature and MHCII^{lo}CD11c^{hi} immature DCs in mesLNs were determined by flow cytometry. (**c,d**) Cryosections of mesLNs from infected chimeras were stained with anti-B220, anti-CD11c and anti-CD4. Scale bar = 400 μm. (**e**) *Cxcl13* expression in mesLN cells were determined by quantitative PCR (mean ± SD of three samples). (**f–g**) The mesLN cells were restimulated with anti-CD3 + BFA for 4 h and the frequencies (**f**) and numbers (**g**) of IL-4^{+} CD4 T cells from the chimeras were determined by ICCS. Data are representative of three independent experiments (mean ± SD of five mice per group, *P<0.001, **P<0.01).